Self-Aligned Microlens-Integrated Vertical-Cavity Surface-Emitting Lasers

Ki Soo Chang, *Student Member, IEEE*, Young Min Song, and Yong Tak Lee

***Abstract*—A novel method for fabricating microlens-integrated vertical-cavity surface-emitting lasers (VCSELs) by selective oxidation of composition-graded digital alloy AlGaAs was developed. Due to the simultaneous formation of a microlens and oxide aperture via single-step oxidation, self-aligned microlens-integrated VCSELs could be fabricated using standard intracavity-contacted VCSEL processing without additional process steps. The output beam from the oxide-buried and oxide-removed AlGaAs microlens-integrated VCSELs was strongly focused to a beam radius of 3.7 and 3.5 μm at a distance of about 25 and 15 μm, respectively, from the surface of the VCSEL.**

***Index Terms*—Digital alloy, microlens, selective oxidation, vertical-cavity surface-emitting laser (VCSEL).**

I. Introduction

MICROLENSES with large numerical aperture are extensively used in optical systems and devices to collimate and focus a diode-laser output beam due to the large output beam divergence of the diode-lasers. In particular, combinations of microlenses with vertical-cavity surface-emitting lasers (VCSELs) have a wide range of applications, including free-space parallel optical interconnects [1], optical memory systems [2], and optical tweezers [3]. However, accurate alignment of microlenses with VCSELs is needed due to the small size of these devices. Mechanical instabilities and high packaging cost are additional concerns that should be considered. As such, microlenses that can be monolithically integrated with VCSELs are strongly in demand for implementing such systems. To date, many different fabrication technologies for monolithic microlens-integrated VCSELs, such as photoresist reflow followed by dry-etching [4], focused ion beam milling [5], and diffusion-limited wet-etching [6], have been developed. However, these methods require multiple process steps for the fabrication of the microlens and an alignment step for lens–laser monolithic integration. Recently, we developed a novel method for fabricating semiconductor microlenses by selective oxidation of composition-graded digital alloy AlGaAs [7]. The most obvious advantage of fabricating microlens-integrated VCSELs using this method is that it allows for self-aligned microlens formation on VCSEL without additional process steps due to the simultaneous formation of a microlens and oxide aperture via single-step oxidation by properly controlling the composition of AlGaAs in the oxidation layer. This technique can also be applicable to the precise control of lens-shaped oxide aperture in VCSEL to reduce scattering loss [8].

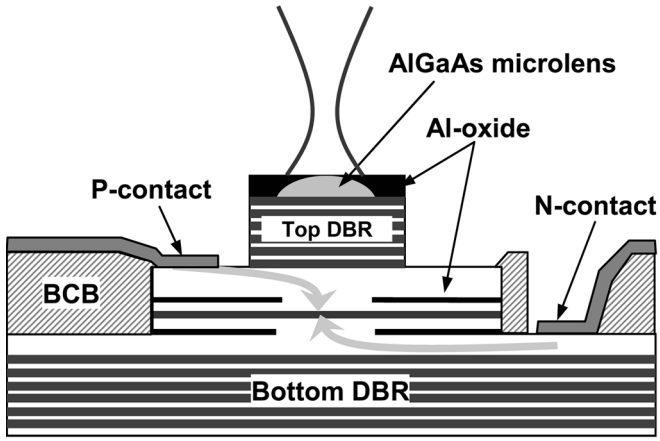

Fig. 1. Schematic diagram of oxide-buried focusing microlens-integrated top-emitting VCSEL.

In this letter, we present the fabrication method and optical performances of self-aligned focusing microlens-integrated VCSELs.

II. Growth and Fabrication

Fig. 1 is a schematic diagram of the proposed microlens-integrated top-emitting VCSEL structure for a focused output beam. In order to experimentally confirm the validity of the proposed concept, 980-nm oxide-confined VCSELs monolithically integrated with semiconductor microlenses formed by selective oxidation of composition-graded AlGaAs were fabricated. All samples presented in this study were grown using DCA P600 solid source molecular beam epitaxy system. Growth rates were calibrated using *in situ* optical reflectometry before every growth run.

The bottom and top distributed Bragg reflector (DBR) mirror consists of 30.5 and 23 pairs of quarter-wavelength-thick GaAs–$Al_{0.88}Ga_{0.12}As$ layers, respectively. The resonator cavity consists of three 80-Å-thick $In_{0.2}Ga_{0.8}As$ quantum wells with 100-Å-thick GaAs barriers surrounded by $Al_{0.3}Ga_{0.7}As$ spacers to form a single wavelength cavity. The cavity is bounded on each side by p- and n-doped $Al_{0.98}Ga_{0.02}As$ oxidation layers followed by $5/4\lambda$-thick p- and n-doped GaAs contact layers. Added on top of the whole VCSEL structure is a 1.3-μm-thick AlGaAs, in which the average Al composition is linearly graded from 0.8 to 0.96 along the growth direction. The chirped short-period superlattice (SPS) of $Al_{0.98}Ga_{0.02}As$ (16-90 ML)/GaAs (4 ML) in 75 steps was used to grade the

Manuscript received July 5, 2006; revised August 10, 2006. This work was supported by MOST through the TND project.

The authors are with the Department of Information and Communications, Gwangju Institute of Science and Technology (GIST), Gwangju 500-712, Republic of Korea (e-mail: ytlee@gist.ac.kr).

Digital Object Identifier 10.1109/LPT.2006.884274

composition of AlGaAs. This SPS technique enables the formation of microlenses using selective oxidation with simple linear composition grading [7]. $Al_{0.98}Ga_{0.02}As$ was used instead of AlAs in SPS because the oxide formed from wet oxidation of $Al_{0.98}Ga_{0.02}As$, rather than AlAs, was reported to be mechanically stable [9] and the slower oxidation rate of $Al_{0.98}Ga_{0.02}As$–GaAs SPS than that of AlAs–GaAs SPS is suitable for the simultaneous formation of a microlens and oxide aperture. The structure was then capped with a 1/4-λ-thick GaAs layer.

After growth, standard intracavity-contacted VCSEL processing was used to fabricate microlens-integrated VCSELs. First, cylindrical mesas of 20 μm in diameter were formed by dry-etching through the outermost GaAs cap layer, composition-graded AlGaAs, and top DBR down to the p-GaAs contact layer using $SiCl_4$-Ar plasma in an inductively coupled plasma etching system. The etching depth was controlled accurately using a laser interferometer, which can provide information about etch depth in real time [10]. Next, cylindrical mesas of 54 μm in diameter, whose centers coincide with the centers of the 20-μm mesas, were defined. The p-GaAs contact layer, two $Al_{0.98}Ga_{0.02}As$ oxidation layers, and the cavity were etched until the n-GaAs contact layer was exposed. The etched samples were oxidized immediately after the etching process in order to avoid natural oxidation. A wet thermal oxidation process for the simultaneous formation of 5-μm-diameter current aperture and oxide-buried microlens was carried out at a temperature of 400 °C for 70 min. After oxidation, benzocyclobutene was spun on the sample and cured at 210 °C for 60 min for passivation. This passivation layer was then partially etched for contact formation. P-contact metal (Ti–Pt–Au) and n-contact metal (Ni–Au–Ge–Ni–Au) were deposited on the p- and n-GaAs contact layer, respectively. The contacts were alloyed for 20 s at 400 °C. After completion of VCSEL processing, the Al-oxide covering the AlGaAs microlens was selectively removed using 1 : 5 KOH (45% w/w) : H_2O solution [11]. Fig. 2(a) shows an optical microscope image of a microlens-integrated VCSEL after Al-oxide removal. The surface profile of the microlens along the line passing through the center of the lens is shown in Fig. 2(b). The radius of curvature of the AlGaAs microlens estimated from the circular fit is 27 μm. The calculated focal lengths of oxide-buried and oxide-removed AlGaAs microlenses obtained using commercial ray tracing software are 23 and 14 μm, respectively. The focal length of the oxide-buried microlens is about 1.6 times longer than that of the oxide-removed AlGaAs microlens. Fig. 2(c) shows a three-dimensional (3-D) surface profile of the microlens-integrated VCSEL measured by confocal microscopy (NanoFocus, μSurf). It can be seen that the surface profile of the microlens is circularly symmetric.

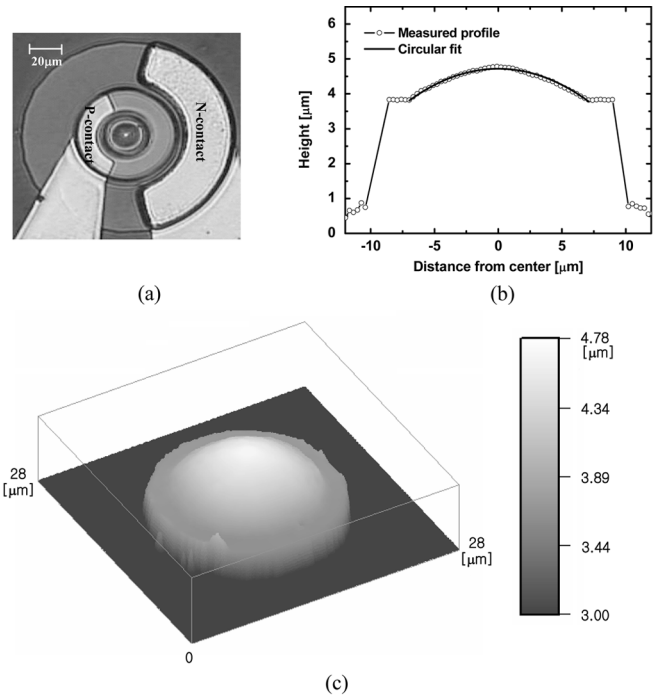

Fig. 2. (a) Microscope image of microlens-integrated VCSEL after Al-oxide removal. (b) Surface profile along the line passing through the center of the microlens. (c) A 3-D surface profile measured by confocal microscopy.

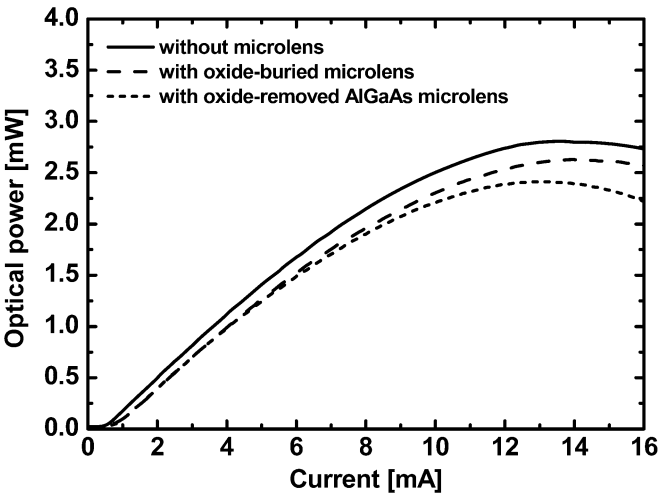

Fig. 3. Light–current characteristics of three 5-μm oxide-apertured VCSELs; without microlens, with oxide-buried AlGaAs microlens, and with oxide-removed AlGaAs microlens.

III. Device Characterization

For direct comparison, three sets of VCSEL devices, i.e., 1) without microlens, 2) with oxide-buried AlGaAs microlens, and 3) with oxide-removed AlGaAs microlens, were prepared from the same VCSEL wafer. VCSELs without microlenses were fabricated after complete selective etching of the outermost GaAs and composition-graded AlGaAs layer using citric acid/H_2O_2 and H_2O/buffered oxide etch [mixture of 7 : 1 NH_4F-HF] solutions, respectively [12]. Fig. 3 shows the light–output characteristics of the fabricated VCSELs measured using an Agilent 4156C semiconductor parameter analyzer and a silicon photodiode with an active diameter of 10 mm. The slight increase of threshold current of the microlens-integrated VCSEL is attributed to the decrease of upper mirror reflectivity by the composition-graded AlGaAs layer on top of the VCSEL structure. The measured maximum output power of the microlens-integrated VCSEL is slightly smaller than that of the VCSEL without microlens due to the larger beam divergence of the microlens-integrated VCSEL after the beam is focused

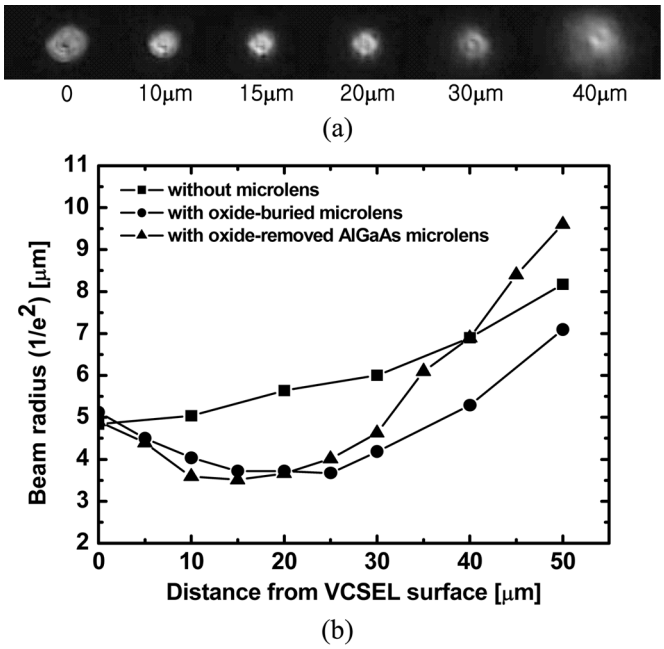

Fig. 4. (a) Output beam images at different distances from top surface of VCSEL integrated with oxide-removed AlGaAs microlens. (b) Measured beam radius versus distance from the top surface of VCSEL. The bias current was 6 mA.

to a beam waist and also due to the limited active area of photodiode.

To verify the focusing function of the microlens, the output beam profiles were measured at different distances from the VCSEL surface, as shown in Fig. 4. The laser beam patterns were magnified by an objective lens and imaged onto a charged-coupled device camera. An image analyzer was used to acquire data. Fig. 4(a) shows images of the output beam from an oxide-removed AlGaAs microlens-integrated VCSEL at different distances from the VCSEL surface. Fig. 4(b) shows the variation of the measured beam radius with distance from the VCSEL surface. The VCSELs were set to operate with a drive current of 6 mA. The output beam from the microlens-integrated VCSEL is focused to a small spot, while the VCSEL without the microlens shows a constantly diverging beam. The minimum beam radius $(1/e^2)$ of 3.5 μm at a distance of about 15 μm was observed for the oxide-removed AlGaAs microlens-integrated VCSEL, thus verifying the strong focusing function of the microlens. For the oxide-buried microlens-integrated VCSEL, the minimum beam radius (3.7 μm) is slightly larger and the distance between the VCSEL surface and the focusing spot (about 25 μm) is longer than that of the oxide-removed microlens-integrated VCSEL due to the effect of Al-oxide covering the AlGaAs lens.

IV. Conclusion

We have developed a simple and robust method for fabricating semiconductor microlenses by selective oxidation of composition-graded AlGaAs grown as chirped SPS. Using this method, we fabricated self-aligned microlens-integrated VCSELs with simultaneous formation of microlenses and oxide apertures via single-step oxidation, which verified the advantages of this method. The fabricated microlens-integrated VCSELs show no significant change of threshold current and output power compared to that of VCSELs without microlenses, while the output beam is strongly focused to a small focusing spot. These microlens-integrated VCSELs can be used in optical systems that require a focused laser beam without additional external optics.

References

[1] A. C. Walker, S. J. Fancey, M. P. Y. Desmulliez, M. G. Forbes, J. J. Casswell, G. S. Buller, M. R. Taghizadeh, J. A. B. Dines, C. R. Stanley, G. Pennelli, A. R. Boyd, J. L. Pearson, P. Horan, D. Byrne, J. Hegarty, S. Eitel, H.-P. Gauggel, K.-H. Gulden, A. Gauthier, P. Benabes, J.-L. Gutzwiller, M. Goetz, and J. Oksman, "Operation of an optoelectronic crossbar switch containing a terabit-per-second free-space optical interconnect," *IEEE J. Quantum Electron.*, vol. 41, no. 7, pp. 1024–1036, Jul. 2005.

[2] K. Goto, Y. Kim, S. Mitsugi, K. Suzuki, K. Kurihara, and T. Hribe, "Microoptical two-dimensional devices for the optical memory head of an ultrahigh data transfer rate and density system using a vertical cavity surface emitting laser (VCSEL) array," *Jpn. J. Appl. Phys.*, vol. 41, pp. 4835–4840, 2002.

[3] A. L. Birbeck, R. A. Flynn, M. Ozkan, D. Song, M. Gross, and S. C. Esener, "VCSEL arrays as micromanipulators in chip-based biosystems," *Biomed. Microdevices*, vol. 5, pp. 47–54, 2003.

[4] E. M. Strzelecka, G. D. Robinson, L. A. Coldren, and E. L. Hu, "Fabrication of refractive microlenses in semiconductors by mask shape transfer in reactive ion etching," *Microelectron. Eng.*, vol. 35, pp. 385–388, 1997.

[5] Y. Fu, "Integration of microdiffractive lens with continuous relief with vertical-cavity surface-emitting lasers using focused ion beam direct milling," *IEEE Photon. Technol. Lett.*, vol. 13, no. 5, pp. 424–426, May 2001.

[6] S. H. Park, Y. Park, H. Kim, H. Jeon, S. M. Hwang, J. K. Lee, S. H. Nam, B. C. Koh, J. Y. Sohn, and D. S. Kim, "Microlensed vertical-cavity surface-emitting laser for stable single fundamental mode operation," *Appl. Phys. Lett.*, vol. 80, pp. 183–185, 2002.

[7] K. S. Chang, Y. M. Song, and Y. T. Lee, "Microlens fabrication by selective oxidation of composition-graded digital alloy AlGaAs," *IEEE Photon. Technol. Lett.*, vol. 18, no. 1, pp. 121–123, Jan. 1, 2006.

[8] E. R. Hegblom, B. J. Thibeault, R. L. Naone, and L. A. Coldren, "Vertical cavity lasers with tapered oxide apertures for low scattering loss," *Electron. Lett.*, vol. 33, pp. 869–871, 1997.

[9] K. D. Choquette, K. M. Geib, H. C. Chui, B. E. Hammons, H. Q. Hou, and T. J. Drummond, "Selective oxidation of buried AlGaAs versus AlAs layers," *Appl. Phys. Lett.*, vol. 69, pp. 1385–1387, 1996.

[10] G. A. Vawter, J. F. Klem, and R. E. Leibenguth, "Improved epitaxial layer design for real-time monitoring of dry etching in III-V compound semiconductor heterostructures with depth accuracy of 8 nm," *J. Vac. Sci. Technol. A*, vol. 12, pp. 1973–1977, 1994.

[11] R. L. Naone and L. A. Coldren, "Tapered air apertures for thermally robust VCL structures," *IEEE Photon. Technol. Lett.*, vol. 11, no. 11, pp. 1339–1341, Nov. 1999.

[12] J. Kim, D. H. Lim, and G. M. Yang, "Selective etching of AlGaAs/GaAs structures using the solutions of citric acid/H_2O_2 and de-ionized H_2 O/buffered oxide etch," *J. Vac. Sci. Technol. B*, vol. 16, pp. 558–560, 1998.